

Supporting Information

Progression Toward Terminal Oxidation of Starch via Hybrid Organic–Enzymatic Bioanode for Renewable Carbohydrate Conversion

Adam Milam^a, Jose Intano, Jr.^{a*}, Shelley D. Minteer^{b*}

* Corresponding authors

^aDepartment of Chemistry, University of Utah

Salt Lake City, Utah 84112

Email: jose.intano@utah.edu

^bDepartment of Chemistry, Missouri University of Science and Technology

Rolla, Missouri 65409

Email: shelley.minteer@mst.edu

Table of Contents

I.	General Information	S2
II.	Electrochemical Cell Configuration	S3
III.	PtKDGA Expression and Purification	S4
IV.	Starch-Iodine Assay	S5
V.	HK/G6PDH and Diaphorase/WST-8 Assay	S6
VI.	Assessment of 4-Amino-TEMPO Compatibility with Starch Hydrolysis	S9
	Enzymes	
VII.	Calculations for Glucose Production from Starch Hydrolysis	S11
VIII.	Calculations for Coulombic Efficiency	S12
IX.	Calculations for Carbon Dioxide Quantification	S12
X.	References	S13

I. General Information

α -Amylase (α -AMY) from *Aspergillus oryzae*, amyloglucosidase (AMG) from *Aspergillus niger*, 4-amino-2,2,6,6-tetramethylpiperidine-1-oxyl (4-amino-TEMPO), adenosine triphosphate (ATP), 2-(*N*-morpholino)ethanesulfonic acid (MES), sodium acetate, glucose, LB (Lennox), magnesium chloride, magnesium phosphate, 3-morpholinopropane sulfonic acid (MOPS), nicotinamide adenine dinucleotide (NADH), nicotinamide adenine dinucleotide phosphate (NADP), nicotinamide adenine dinucleotide phosphate (NADPH), isopropyl- β -D-thiogalactopyranoside (IPTG), potassium iodide, sodium phosphate, iodine, and water-soluble tetrazolium (2-(2-methoxy-4-nitrophenyl)-3-(4-nitrophenyl)-5-(2,4-disulfophenyl)-2H-tetrazolium monosodium salt, WST-8), were used as received from Sigma-Aldrich while 1% (w/v) aqueous starch solution was purchased from Carolina Biological. 18-Ohm Millipore Milli-Q water was used for all solutions. Diaphorase from microorganism (DAD-311) was supplied by Toyobo USA.

A 1% (w/v) aqueous starch solution was selected to achieve final glucose concentrations in the millimolar (mM) range. This starch solution contains 0.5% methylparaben, which was determined to exhibit minimal reactivity with 4-amino-TEMPO under the electrochemical conditions employed. A Benedict's assay, using copper sulfate, sodium citrate, and sodium carbonate, was initially used to evaluate for rapid glucose detection; however, it did not provide sufficient precision. Detectable differences in absorbance required glucose concentration changes of at least 2 mM, and glucose concentrations below 1 mM could not be reliably detected.

The sealed chamber used for CO₂ detection was highly sensitive to ambient CO₂, including exhaled breath. Accordingly, care was taken to minimize CO₂ contamination from ambient CO₂ during chamber assembly, and sufficient time was allowed for the sensor to equilibrate. When the

chamber was opened to atmosphere, a minimum equilibration period of five minutes was observed, and experiments were initiated only after the CO₂ concentration (ppm) stabilized.

II. Electrochemical Cell Configuration

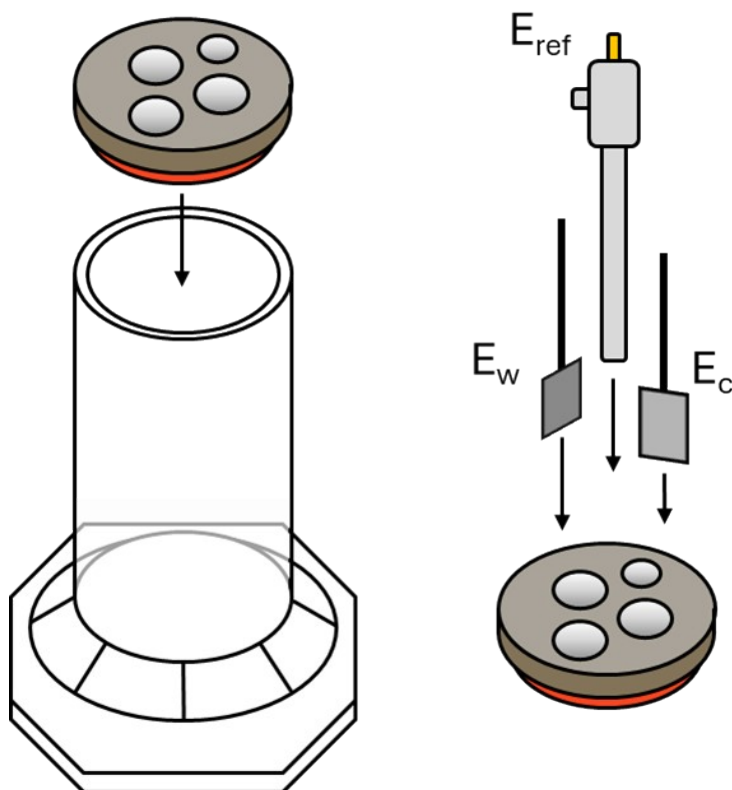


Figure S1. Pine Instruments low-volume electrochemical cell with platinum mesh counter electrode (CE), a saturated calomel electrode (SCE) reference electrode (RE), 3-mm diameter glassy carbon working electrode (WE) for cyclic voltammetry, and a 1-cm² carbon paper working electrode for bulk electrolysis.

Pine Instruments low-volume electrochemical cells (AF01CKT1006) were used for all experiments (10 mL volume, 68 mm hex base, 25 mm cell height). Glassy carbon electrodes were sourced from CH Instruments (CHI104). AvCarb MGL 190 carbon paper electrodes (Fuel Cell

Store) were cut to a geometric area of 1 cm² and were wax treated according to a previously reported procedure.¹

III. PtKDGA Expression and Purification

2-Keto-3-deoxygluconate aldolase from *Picrophilus torridus* (ptKDGA; Uniprot Q6KZI8), bearing a C-terminal 6xHis-tag, was ordered from GenScript and cloned into pET28a(+) between the *NdeI* and *XhoI* restriction sites. The resulting plasmid was transformed into *E. coli* BL21(DE3)pLysE. Transformed *E. coli* cells were plated onto LB agar plates containing 100 µg/mL kanamycin and incubated at 37 °C for 18 hours. Single colonies were used to inoculate starter cultures (44 mL media in 250 mL flasks), which were grown for 24 hours at 37 °C with shaking at 150 rpm. Subsequently, 10 mL of starter culture was used to inoculate each growth flask, and cell growth was monitored by measuring the optical density at 600 nm (OD₆₀₀) at 30-minute intervals. Protein expression was induced at an OD₆₀₀ of 0.5 by addition of IPTG (1 mM), and cultures (1 L LB in 3 L baffled Corning Erlenmeyer flasks, Fernbach design) were incubated at 18 °C with shaking at 150 rpm for 18 hours. Cells were pelleted (800 mL per bottle, 15 kxg, 15 minutes, Sorvall Lynx 6000 centrifuge), flash-frozen in liquid nitrogen, and stored at –80 °C until purification.

Purification of ptKDGA was adapted from a modified ssKDGA protocol, which was originally based on the work of Buchannan and co-workers.^{2,3} Approximately 4 grams of frozen cell pellets were resuspended in lysis buffer (100 mL, 50 mM Tris-HCl, pH 8.0) with two cOmplete™ EDTA-free protease inhibitor tablets (Roche) and lysozyme (1 mg/mL). Cells were lysed by probe sonication (6 seconds on 20 seconds off, total 10 minutes, 40% power) in a sonication beaker, with stirring in an ice-water bath using a Fisherbrand Model 505 sonicator (Qsonica c1334, ½" probe),

followed by two passes of French press homogenizer (Microfluidics M-110P, 138 MPa). The lysate was clarified by centrifugation (15 kxg, 60 minutes) and loaded onto a Ni-NTA affinity column (HisPrep 16/10 FF, 20 mL; Ni Sepharose 6 Fast Flow, Cytiva) using a GE ÄKTA Pure 25 FPLC system. The column was washed with 5% elution buffer, and the protein was eluted using a linear gradient from 5% to 100% elution buffer (500 mM potassium chloride, 250 mM imidazole, 50 mM potassium phosphate, pH 8.0), with fractions collected using an F9-R fraction collector. Eluted protein was concentrated using a centrifugal filter unit (Amicon Ultra-15, 10 kDa MWCO) and buffer-exchanged with phosphate buffer (50 mM, pH 8.0; 15 mL total). The purified enzyme was aliquoted (200 μ L), flash-frozen in liquid nitrogen, and stored at -80 °C. Protein purity was assessed by SDS-PAGE.

IV. Starch-Iodine Assay

Starch concentration was quantified using the starch-iodine assay described in the main text (**Experimental Section 2.1**). The assay was linear from 0 to 0.008% (w/v) starch (**Figure S2**), with no detectable interference from other reagents; accordingly, all samples were diluted 20-fold prior to analysis to ensure absorbance values remained within the linear range of detection.

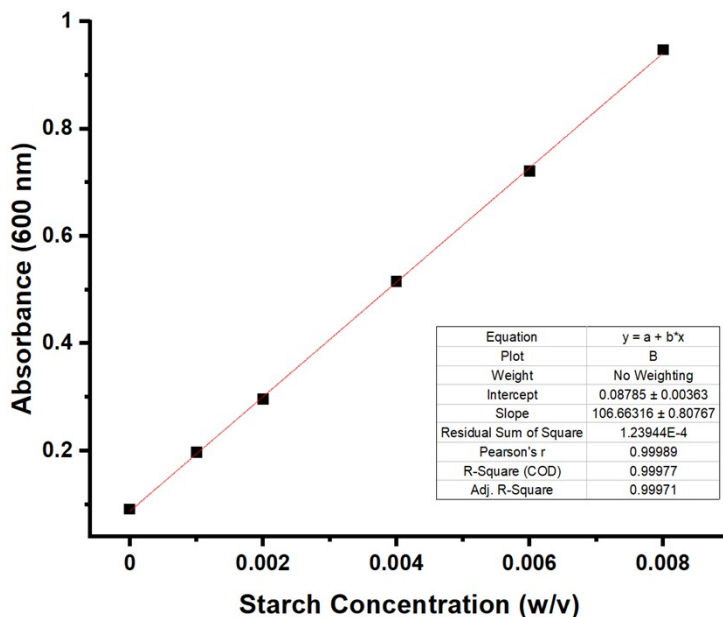


Figure S2. Calibration curve for the starch-iodine assay over a concentration range of 0–0.008% (w/v) starch, corresponding to 0–5 mM glucose equivalents (based on complete hydrolysis).

V. HK/G6PDH and Diaphorase/WST-8 Assay

Glucose concentrations were quantified using the coupled hexokinase/glucose-6-phosphate dehydrogenase (HK/G6PDH) assay described in the main text (**Experimental Section 2.2**). WST-8 exhibited a linear absorbance response to NADPH concentration over two ranges: 0–60 μ M glucose equivalents when monitored at 450 nm, and 100–1000 μ M glucose equivalents when monitored at 600 nm. Statistical analysis was performed as described in the main text.

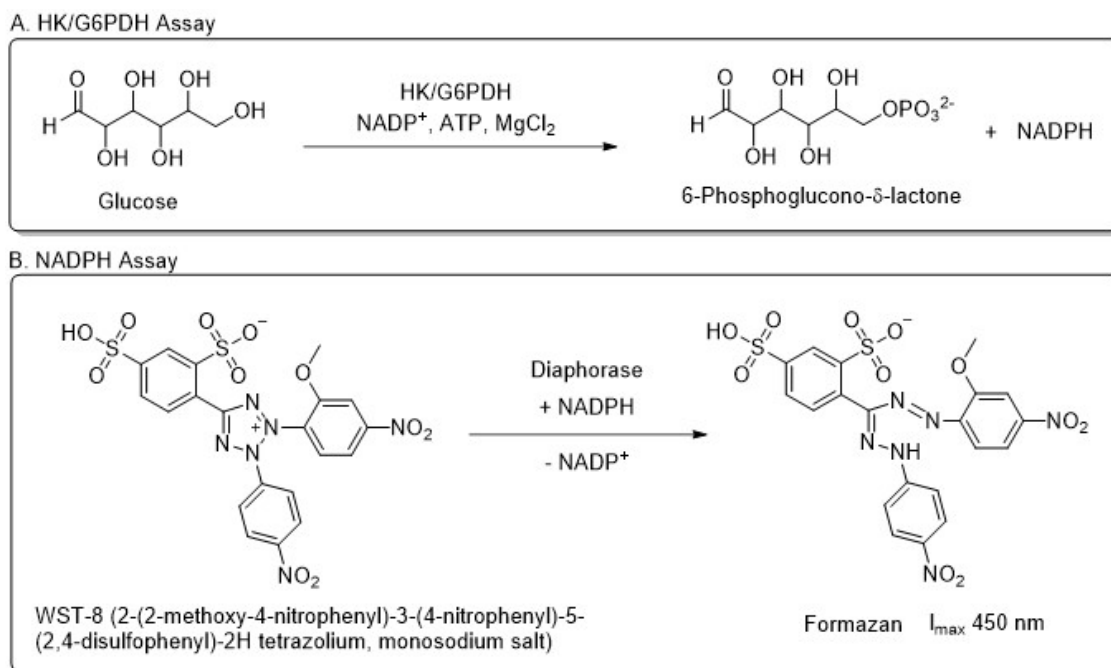


Figure S3. (A) Schematic of the glucose detection assay using hexokinase and glucose 6-phosphate dehydrogenase, and (B) NADPH detection assay using diaphorase and WST-8.

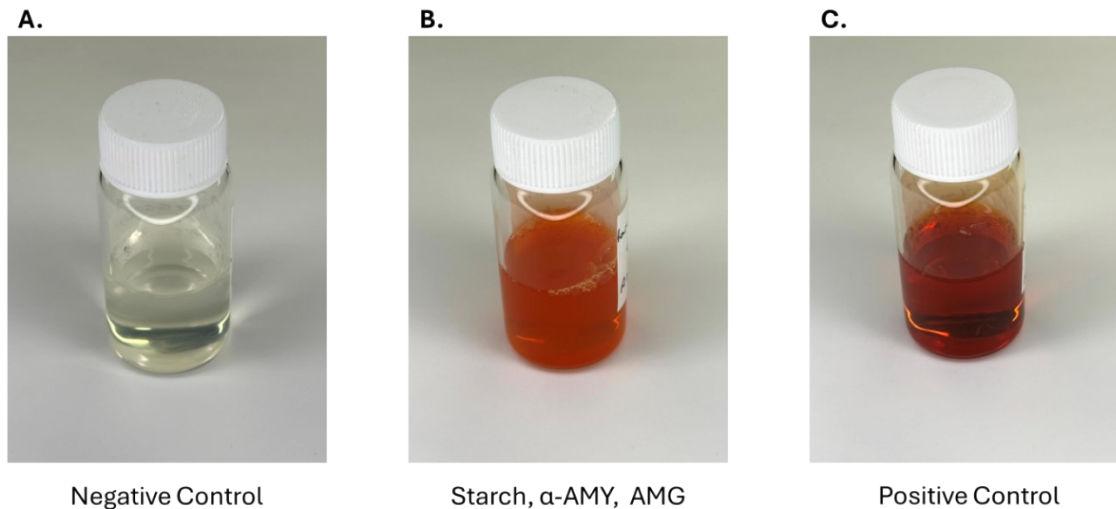


Figure S4. Photographs of (A) starch subjected to the HK/G6PDH, diaphorase, and WST-8 assay, (B) starch treated with α -AMY and AMG, followed by the HK/G6PDH, diaphorase, and WST-8 assay, and (C) glucose subjected to the HK/G6PDH, diaphorase, and WST-8.

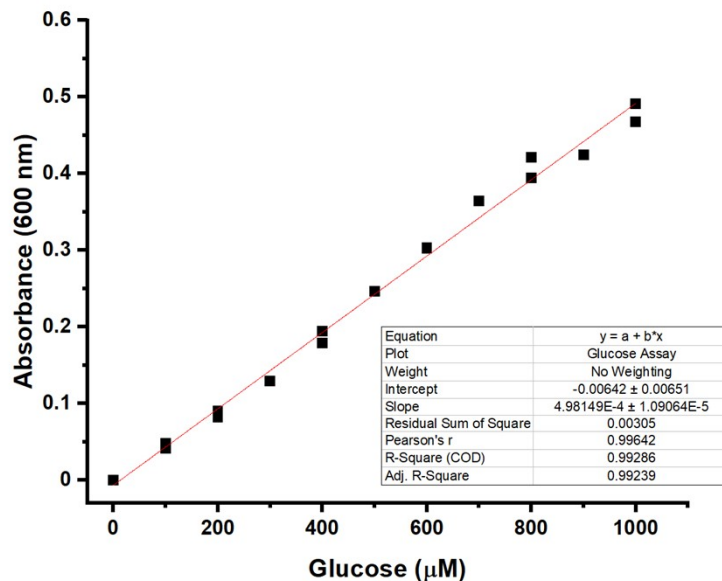


Figure S5. HK/G6PDH assay response monitored via WST-8 absorbance at 600 nm.

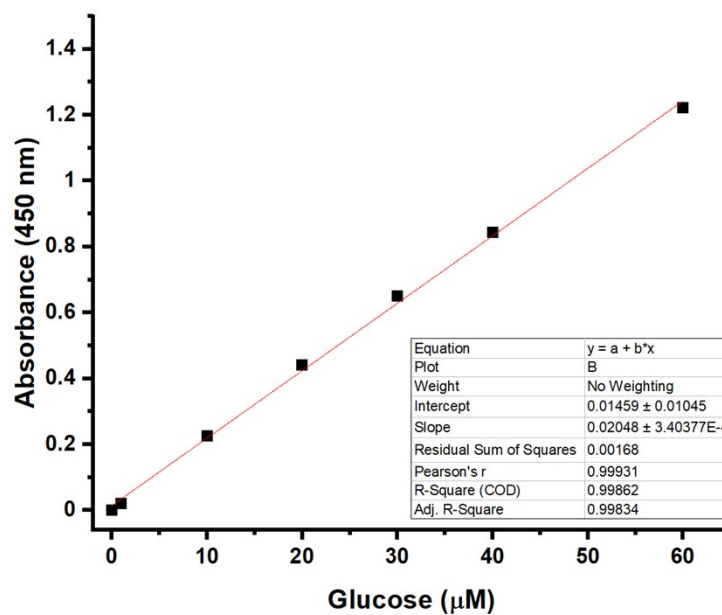


Figure S6. HK/G6PDH assay response monitored via WST-8 absorbance at 450 nm.



Figure S7. Photographs of control HK/G6PDH assay (left), 20-fold diluted starch hydrolysate obtained at pH 5.2 after 1 hour at room temperature (center), and 20-fold diluted starch hydrolysate obtained at pH 5.2 after 1 hour at 60 °C (right).

VI. Assessment of 4-Amino-TEMPO Compatibility with Starch Hydrolysis Enzymes

Control experiments were conducted to evaluate potential interactions between 4-amino-TEMPO and the starch hydrolysis enzymes used in this study. Preliminary experiments revealed that an original liquid α -AMY stock contained a low molecular weight contaminant that reacted with 4-amino-TEMPO, even at relatively low enzyme loadings (2 U). To eliminate this source of interference, a substitute lyophilized α -AMY preparation was used for all subsequent experiments. The lyophilized α -AMY preparation exhibited measurable electrochemical effects only at enzyme loadings substantially higher than those used under the operational conditions (red trace, **Figure S8**). Specifically, addition of 120 U α -AMY to a solution containing 5 mM 4-amino-TEMPO resulted in a 9% increase in peak oxidation current density and a 43% increase in diffusion-limited current density, while producing only a 1% decrease in peak reduction current density. Similarly,

addition of 120 U of AMG resulted in an 18% increase in diffusion-limited current density (blue trace, **Figure S8**). However, both enzymes were employed at only 6 U during starch hydrolysis experiments. Consequently, any enzyme-mediated perturbation of the 4-amino-TEMPO redox response under the conditions used in this study was considered negligible. Although post-hydrolysis centrifugal filtration was later implemented to improve glucose retention and electrochemical reproducibility (see main text), filtration was not required to mitigate direct redox interference from either α -AMY or AMG.

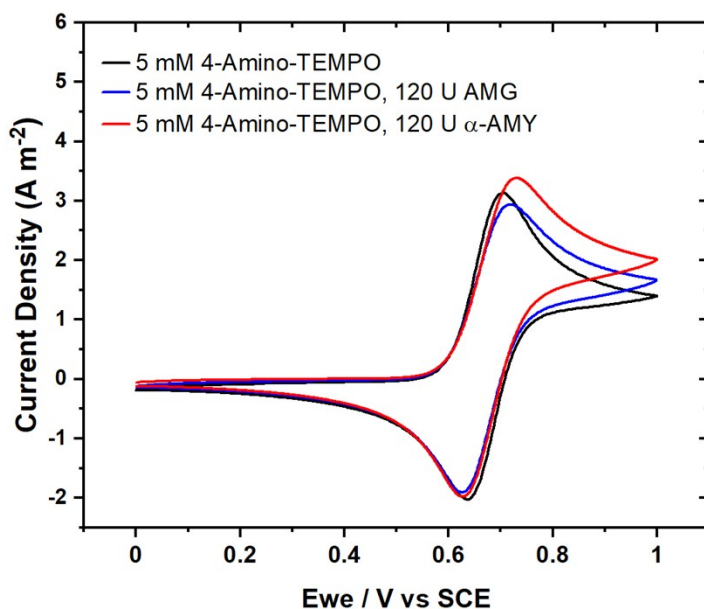


Figure S8. Cyclic voltammograms of 5 mM 4-amino-TEMPO in the absence (black) and presence of 120 U AMG (blue), and 120 U α -AMY (red). Measurements were performed using a 3 mm glassy carbon working electrode, platinum mesh counter electrode, and SCE reference electrode in 40 mM citrate buffer (pH 5.2) at a scan rate of 10 mV/s.

VII. Calculations for Glucose Production from Starch Hydrolysis

Absorbance values obtained from 20-fold dilution of the hydrolysate solution following one hour hydrolysis at 60 °C in 40 mM citrate buffer (pH 5.2) with 6 U each of α -AMY and AMG were: 0.219, 0.220, 0.242, 0.221, 0.210

Glucose concentrations were determined using the calibration curve derived in Fig. S5 according to the following equation:

$$\text{Absorbance} = 0.000496 * [\mu\text{M Glucose}] - 0.00642$$

Calculated glucose concentrations for the five trials were: 9.09, 9.13, 10.02, 9.17, and 8.73 mM.

Mean Glucose Concentration: $\bar{x} = 9.23$ mM

Sample Standard Deviation: $s = 0.476$ mM

The 95% confidence interval was calculated using $\bar{x} \pm t\left(\frac{s}{\sqrt{n}}\right)$, yielding a glucose concentration of 9.23 ± 0.59 mM. Based on the initial starch loading, the conversion of starch-derived glucose equivalents following one hour hydrolysis at 60 °C in 40 mM citrate buffer (pH 5.2) with 6 U each of α -AMY and AMG was determined to be $92.3 \pm 5.9\%$.

VIII. Calculations for Coulombic Efficiency

Coulombic efficiency was determined from chronoamperometry performed at 0.85 V vs SCE for 24 hours using the complete catalyst system consisting of 5 mM 4-amino-TEMPO, 10 U ptKDGA, and 10 U OxDC with filtered starch hydrolysate. Theoretical charge values were calculated based on glucose consumption measured using the HK/G6PDH assay, assuming complete oxidation of glucose to CO₂ (24 electrons per glucose equivalent). Coulombic efficiencies were determined from the ratio of experimentally measured cumulative charge to the calculated theoretical charge.

Based on three independent trials, the average coulombic efficiency was determined to be $36.1 \pm 8.1\%$ (95% CI, $n = 3$).

Table S1. Coulombic efficiency calculations based on glucose consumption measured by the HK/G6PDH assay and cumulative charges obtained during the 24-h chronoamperometry.

Trial	Cumulative Charge (C)	Glucose Conversion (%)	Glucose Consumed (mol)	Theoretical Charge (C)	Coulombic Efficiency (%)
1	7.517	11.4	8.38×10^{-6}	19.5	38.6
2	6.424	10.1	7.45×10^{-6}	17.3	37.1
3	8.412	15.2	1.12×10^{-5}	25.9	32.5

IX. Calculations for Carbon Dioxide Quantification

Carbon dioxide concentrations were measured using the headspace probe within the sealed chamber as described in **Experimental Section 2.3** of the main text. Changes in CO_2 concentration were monitored during the six hours of chronoamperometry performed at 0.85 V vs SCE. No further measurable increase in CO_2 concentration was observed beyond this period despite continued electrolysis; therefore, only the initial six-hour interval was used for CO_2 quantification. The fraction of consumed glucose detected as CO_2 was estimated from the measured increase in chamber CO_2 concentration and the quantity of glucose consumed during electrolysis.

Sealed chamber volume = 0.04 m^3

1 ppm increase in CO_2 concentration = $1.59 \times 10^{-6} \text{ mol CO}_2$

Complete oxidation of 1 mol glucose = 6 mol CO_2

Table S2. Estimated percentage of consumed glucose detected as CO₂ during the first six hours of chronoamperometry at 0.85 V vs SCE using the complete catalyst system.

Trial	Glucose Consumed (mol)	CO ₂ Produced (mol)	Glucose Converted to CO ₂ (%)
1	8.38 x 10 ⁻⁶	4.77 x 10 ⁻⁶	10.7
2	7.45 x 10 ⁻⁶	3.18 x 10 ⁻⁶	8.1
3	1.12 x 10 ⁻⁵	6.36 x 10 ⁻⁶	10.4

Mean percent conversion: $\bar{x} = 9.73\%$

Sample Standard Deviation: $s = 1.40\%$

Based on the measured glucose consumption and observed CO₂ evolution, approximately 9.73 ± 3.48% of the consumed starch-derived glucose equivalents were detected as CO₂ during the first six hours of chronoamperometry using the complete catalyst system containing 5 mM 4-amino-TEMPO, 10 U ptKDGA, and 10 U OxDC. Because no significant increase in CO₂ concentration was observed after the initial six-hour monitoring period, this value represents a lower-bound estimate of carbon mineralization during cascade operation.

X. References

1. R. Gerulskis, S. D. Minteer, *ECS Adv.*, 2023, **2**, 035501. DOI: 10.1149/2754-2734/ace203.
2. A. Milam, R. Gerulskis, J. Intano, S. D. Minteer, *ACS Catal.*, 2025, **15**, 11013–11021. DOI: 10.1021/acscatal.5c02892.
3. C. L. Buchanan, H. Connaris, M. J. Danson, C. D. Reeve, D. W. Hough, *Biochem. J.*, 1999, **343**, 563–570. DOI: 10.1042/bj3430563.